

**NASA
Technical
Paper
2414**

C.2
January 1985

Downwash in the Plane of Symmetry of an Elliptically Loaded Wing

James D. Phillips

**TECHNICAL REPORTS
FILE COPY**

Property of U. S. Air Force
AEDC LIBRARY
F40600-81-C-0004

NASA

**NASA
Technical
Paper
2414**

1985

Downwash in the Plane of Symmetry of an Elliptically Loaded Wing

James D. Phillips

*Ames Research Center
Moffett Field, California*

NASA

National Aeronautics
and Space Administration

Scientific and Technical
Information Branch

SYMBOLS

AR	aspect ratio, the ratio of wingspan to average chord
c	wing chord
C_l	local lift coefficient
C_{l_α}	local lift slope
C_L	wing lift coefficient
$E(k)$	complete elliptic integral of the second kind with parameter, k (see eq. (14))
h	perpendicular distance between a vortex line and a point (see fig. 2)
r	distance from a point in the plane of symmetry to the lifting line, $\sqrt{x^2 + z^2}$
s	wing semispan
V	free-stream velocity
w_i	induced downwash velocity at the lifting line; downwash is defined as negative
w_p	induced downwash velocity at a point P in the plane of symmetry; downwash is defined as negative
x	distance <i>downstream</i> from the lifting line (see fig. 3)
y	distance to the <i>right</i> along the wingspan (see fig. 3), also the semispan of a differential horseshoe vortex (see fig. 1)
y_0	integration variable referencing a span location
z	distance <i>above</i> the lifting line (see fig. 3)
α	angle of attack

α_i	angle of attack induced at the lifting line, $\alpha_i = C_L/\pi AR$ for an elliptically loaded wing
Γ	local circulation
ϵ	downwash angle, $\epsilon \approx w/V$; downwash is defined as negative
$\bar{\epsilon}$	normalized downwash, ϵ/α_i , downwash is defined as negative
$\bar{\epsilon}_1, \bar{\epsilon}_2, \bar{\epsilon}_3$	normalized downwash integrals (see eqs. (17))
ζ	dimensionless vertical coordinate, z/s
η	dimensionless spanwise coordinate, y/s
θ_p	stagger angle (see fig. 3); note that $\theta_p > 0$ downstream and $\theta_p < 0$ upstream
θ_1, θ_2	angles between a vortex line segment endpoint and an arbitrary point (see fig. 2)
$\Lambda_0(\beta, k)$	Heuman's lambda function, tabulated in reference 8
ξ	dimensionless streamwise coordinate, x/s
$\Pi(\alpha^2, k)$	complete elliptic integral of the third kind
ρ	dimensionless radius from the lifting line to a point P in the plane of symmetry, r/s
ϕ_p	gap angle (see fig. 3); note that $(\tan \phi_p)^{-1}$ is the gap ratio, $\zeta = z/s$
ψ_p	angle between the wing tip and the midspan viewed from a point P in the plane of symmetry (see fig. 3)

DOWNWASH IN THE PLANE OF SYMMETRY
OF AN ELLIPTICALLY LOADED WING

James D. Phillips

Ames Research Center

SUMMARY

A closed-form solution for the downwash in the plane of symmetry of an elliptically loaded line is given. This theoretical result is derived from Prandtl's lifting-line theory and assumes that (1) a three-dimensional wing can be replaced by a straight lifting line, (2) this line is elliptically loaded, and (3) the trailing wake is a flat-sheet which does not roll up. The first assumption is reasonable for distances greater than about 1 chord from the wing aerodynamic center. The second assumption is satisfied by any combination of wing twist, spanwise camber variation, or planform that approximates elliptic loading. The third assumption is justified only for high-aspect-ratio wings at low lift coefficients and downstream distances less than about 1 span from the aerodynamic center.

It is shown, however, that assuming the wake to be fully rolled up gives downwash values reasonably close to those of the flat-sheet solution derived in this paper. The wing can therefore be modeled as a single horseshoe vortex with the same lift and total circulation as the equivalent elliptically loaded line, and the predicted downwash will be a close approximation independent of aspect ratio and lift coefficient.

The flat-sheet equation and the fully rolled up wake equation are both one-line formulas that predict the upwash field in front of the wing, as well as the downwash field behind it. These formulas are useful for preliminary estimates of the complex aerodynamic interaction between two wings (i.e., canard, tandem wing, and conventional aircraft) including the effects of gap and stagger.

INTRODUCTION

The downwash field that surrounds a wing has been a topic of study since the first practical airplane because of its critical effect on longitudinal stability. Much of the past research was concerned with determining the downwash at the normal location of the horizontal tail on a conventional aircraft. Unconventional configurations, that is, canards and tandem-winged aircraft, allow increased flexibility for the designer but require a broader knowledge of the wing downwash field to predict the longitudinal stability.

Most of the past theoretical investigations of downwash are based on Prandtl's lifting-line theory, in which the wing is replaced by a line of superposed elemental "horseshoe" vortices. The sum of the horseshoe vortices is chosen to match the span loading of the wing. The span loading, in turn, is a function of planform shape, airfoil, and twist distribution and, in general, requires the solution of an integral equation. The solution is particularly simple if the loading is elliptical, in which case the downwash is uniform across the span.

Once the span-loading distribution is established, the downwash is obtained by integrating over the span the contributions of each elemental horseshoe vortex to the induced velocity at a specified point in space. Only a few special cases of this integral have been solved analytically. Exact solutions for elliptic loading have been given for the longitudinal axis ($y = 0, z = 0$) and the lateral ($y-z$) plane by Glauert (ref. 1, pp. 164-166) and others. Silverstein and Katzoff (ref. 2) performed the integration numerically for various taper ratios, as well as elliptic loading, and presented the results in graphical form for use in design. These results are only shown, however, for the usual position of a horizontal tail behind a wing.

This paper presents the exact solution for the downwash in the entire plane of symmetry ($x-z$ plane) of an elliptically loaded line. The solution is a one-line formula requiring only a calculator and tables of elliptic integrals to apply. It is formulated in terms of intuitive geometric angles, providing a mental picture of the physical situation.

This is a valuable feature because significant trends can be seen immediately.

Acknowledgment is gratefully made to Dr. R. T. Jones for his valuable comments on this paper. Dr. Heinz Erzberger also deserves a special note of thanks for his help in translating reference 7.

LIFTING-LINE THEORY

The basic lifting-line theory is described in most elementary texts on aeronautics (e.g., ref. 3, pp. 131-136). It is presented here for completeness and to introduce a few basic equations which are needed in the next section.

The fundamental idea is to replace a wing of finite span by an infinite sum of differential line vortices. According to Helmholtz's laws, these line vortices must be closed loops. Prandtl builds the wing-circulation distribution from rectangular-shaped vortex loops he named "horseshoe" vortices (see fig. 1).

Each horseshoe vortex is made up of four line segments forming a closed loop. The segment of this loop at the lifting line is called the bound vortex; the sides of the loop, which extend to infinity downstream, are called the trailing vortices; and the closing segment at infinity is called the starting vortex.

The velocity induced by a differential vortex-line segment at a specified point is given by the Biot-Savart law:

$$d\vec{w} = \frac{\Gamma}{4\pi} \frac{d\vec{l} \times \hat{r}}{|\vec{r}|^2} \quad (1)$$

where \vec{w} is the velocity induced by the differential vortex segment, $d\vec{l}$; Γ is the circulation around the vortex segment; and \vec{r} is a position vector from the vortex segment to the point of interest.

Since horseshoe vortices are made solely of straight-line segments, it will prove useful to integrate the Biot-Savart law for the velocity induced

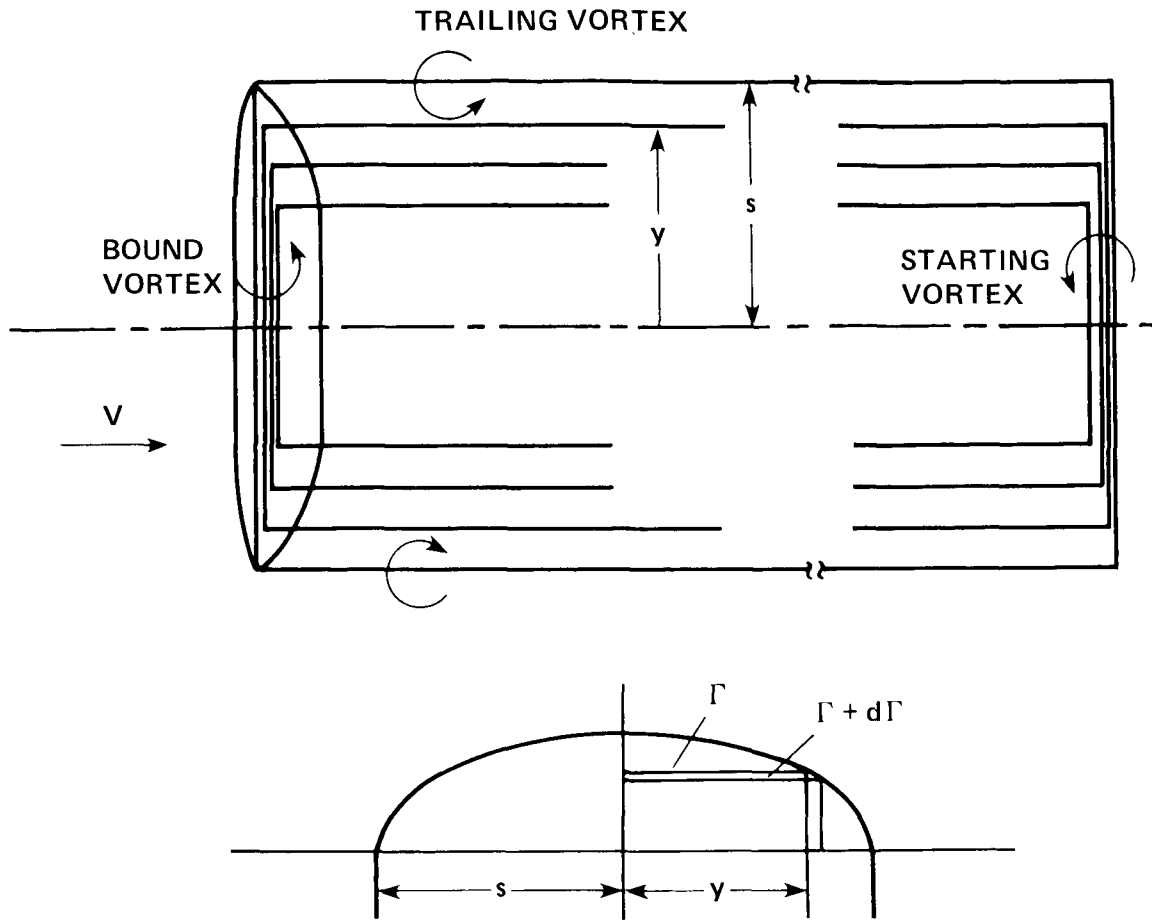


Figure 1. - Prandtl's lifting line theory.

by a generic straight-line segment at a point, P :

$$|\vec{w}_p| = \frac{\Gamma}{4\pi h}(\cos \theta_1 + \cos \theta_2) \quad (2)$$

where h , θ_1 , and θ_2 are defined in figure 2. For a semi-infinite vortex line segment (such as a trailing vortex), $\theta_1 = \frac{\pi}{2}$, $\theta_2 = 0$, and $w_p = \Gamma/4\pi h$.

It can be shown that the induced downwash at a point on the span depends only on the trailing vortex system. Applying the Biot-Savart

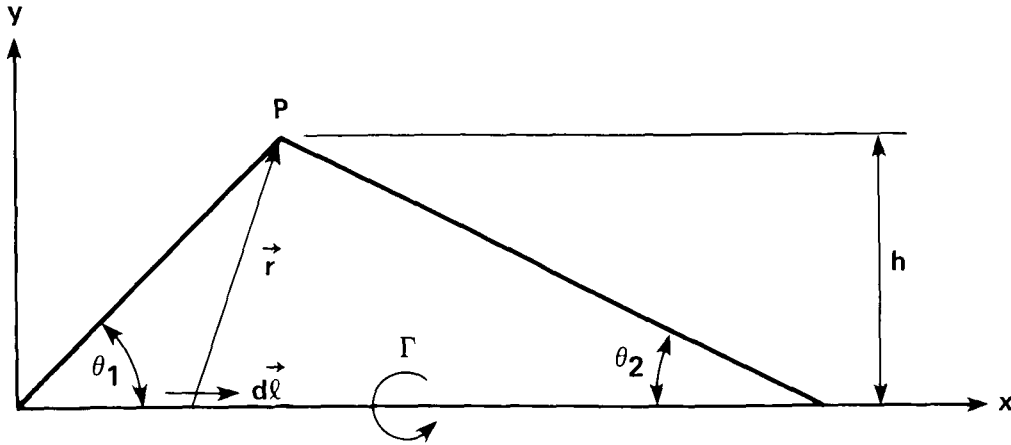


Figure 2. - Biot-Savart law for a straight line segment.

law (eq. (2)) for the trailing vortex system of a differential horseshoe vortex (two semi-infinite vortex lines) and integrating across the span, the induced velocity and the induced angle of attack (approximately) are given by

$$\alpha_i(y) \approx \frac{w_i}{V} = \frac{1}{4\pi V} \int_{-s}^s \frac{d\Gamma(y_0)}{y - y_0} \quad (3)$$

Assuming that the flow is locally two dimensional, the section lift coefficient at a spanwise location is given by

$$C_l(y) = C_{l_\alpha} [\alpha - \alpha_i(y)] \quad (4)$$

In general, α in equation (4) can also be a function of span; for example, if the wing is twisted.

The circulation at y is related to the lift coefficient by the Kutta-Joukowski theorem:

$$\Gamma(y) = \frac{1}{2} c(y) C_l(y) V \quad (5)$$

where c is the section chord at span location y .

Equations (3)–(5) can be combined into a single integral equation called the Prandtl lifting-line equation. The standard solution of this equation for

an arbitrary load distribution is a Fourier series — a tedious calculation. Prandtl discovered an elegant solution which also produces the minimum induced drag for a given span and total lift. This is the case of elliptic loading:

$$\Gamma = 4s \frac{C_L}{\pi AR} V \sqrt{1 - \left(\frac{y}{s}\right)^2} \quad (6)$$

After substituting equation (6) into equation (3) and performing the indicated integration it is seen that the induced angle of attack is a constant over the span equal to $C_L/\pi AR$. When this result is substituted into equation (4), it is seen that the local lift coefficient is also a constant along the span. Equation (5) now shows that the circulation is only a function of spanwise chord distribution, so that a straight, untwisted wing of elliptic planform will give the desired loading.

The assumptions made are that the chord is small relative to the span, that the span is straight, and that the wing loading is symmetric about the midpoint. The first assumption implies that the velocity calculation is inaccurate very close to the chord. Silverstein et al. (ref. 4, p. 3) show that for the two-dimensional case, the lifting-line approximation is very accurate at a distance more than 1 chord length behind the trailing edge. It is reasonable to assume this will be true upstream as well, since the two-dimensional solution is antisymmetric longitudinally about the span line.

A further assumption is that the trailing vortices extend downstream to infinity as straight lines. This assumption is quite accurate for the purpose of calculating the span load-distribution, because the induced velocity is determined on the span line. For a downwash calculation behind the airfoil, this assumption is less justified, because the vortex sheet is, in reality, unstable and rolls up into two discrete vortex cores.

Experimental investigations of downwash have been only qualitatively useful in validating these assumptions because of the difficulty in correcting for the effects of wind-tunnel walls. One of the earliest studies was done in 1925 by Fage and Simmons (ref. 5), who measured the downwash in

various lateral planes both in front of and behind a rectangular wing. In 1936, Muttray (ref. 6) measured the downwash behind both rectangular and elliptical wings in the plane of symmetry and compared the results with various approximate theories. And in 1938, Silverstein et al. (ref. 4), in validating the method used to produce the design charts of reference 2, measured the downwash in three lateral planes behind a 45.75-ft-span, 2:1-tapered wing placed in the full-scale wind tunnel at NASA Langley Research Center. The Langley results are qualitative because no wind-tunnel correction was attempted. It is demonstrated, however, that the rolling up process is far from complete at the normal position of a horizontal tail.

DOWNWASH INTEGRAL

Once a solution for the Prandtl lifting-line equation is found, that is, once the load distribution is known, the downwash at an arbitrary point is calculated by integrating the Biot-Savart law over the entire vortex field. This is the basis for reference 2, which presents downwash charts for use in design. In general, the problem is only tractable if it is treated numerically. Exact solutions are known for only a few special cases involving elliptic loading.

The assumption of a uniform load distribution, that is, a single horseshoe vortex with an appropriate strength, is often used to approximate the downwash because it is simple and spans the entire three-dimensional space. The uniform span loading does not, however, go continuously to zero at the wing tips as it must for real wings. Fortunately, any physically realizable load distribution can be represented as an integral of differential horseshoe vortices.

Applying equation (2) for a single horseshoe vortex with semispan y at a point (x, z) in the plane of symmetry gives

$$|\vec{w}| = -\frac{\Gamma}{2\pi y} \left[\frac{x}{\sqrt{x^2 + y^2 + z^2}} \left(\frac{y^2}{x^2 + z^2} + \frac{y^2}{y^2 + z^2} \right) + \frac{y^2}{y^2 + z^2} \right] \quad (7)$$

Note that the origin is at midspan in the plane of symmetry, x is

downstream, and z is up in the plane of symmetry.

For a known loading, Γ is replaced by $-\frac{d\Gamma}{dy}dy$. Differentiating the elliptic loading expression (eq. (6)) gives

$$-\frac{d\Gamma}{dy} = 4\alpha_i V \frac{\frac{y}{s}}{\sqrt{1 - \left(\frac{y}{s}\right)^2}} \quad (8)$$

where $\alpha_i = C_L/\pi AR$.

Defining $\bar{\epsilon} = \epsilon/\alpha_i$ where $\epsilon \approx w/V$, substituting $-\frac{d\Gamma}{dy}dy$ from equation (8) for Γ in equation (7), and integrating over the semispan yields

$$\bar{\epsilon} = -\frac{2}{\pi s} \int_0^s \frac{dy}{\sqrt{1 - \left(\frac{y}{s}\right)^2}} \left[\frac{x}{\sqrt{x^2 + y^2 + z^2}} \left(\frac{y^2}{x^2 + z^2} + \frac{y^2}{y^2 + z^2} \right) + \frac{y^2}{y^2 + z^2} \right] \quad (9)$$

The exact solution of equation (9) is the subject of this paper.

The solutions for two special cases of equation (9) have been given by Glauert and others. The first special case is along the z -axis for which equation (9) simplifies to

$$\bar{\epsilon} = -\frac{2}{\pi s} \int_0^s \frac{dy}{\sqrt{1 - \left(\frac{y}{s}\right)^2}} \left[\frac{y^2}{y^2 + z^2} \right] \quad (10)$$

By a trigonometric substitution, the solution for equation (10) (ref. 1, p. 163) is

$$\bar{\epsilon} = -\left[1 - \frac{|z|}{\sqrt{s^2 + z^2}} \right] \quad (11)$$

Note that in equation (11), $\bar{\epsilon}$ goes to zero for $z = \pm\infty$ and unity ($\epsilon = \alpha_i$) for $z = 0$.

The second special case is along the x -axis. Equation (9) simplifies to

$$\bar{\epsilon} = -\frac{2}{\pi s} \int_0^s \frac{dy}{\sqrt{1 - (y/s)^2}} \left[\frac{\sqrt{x^2 + y^2}}{x} + 1 \right] \quad (12)$$

Again, Glauert gives the solution (ref. 1, p. 166):

$$\bar{\epsilon} = -\left[1 + \operatorname{sgn}(x) \frac{2}{\pi} \frac{E(k)}{\sqrt{1 - k^2}} \right] \quad (13)$$

where $k^2 = s^2/(x^2 + s^2)$ and $E(k)$ is the complete elliptic integral of the second kind defined by

$$E(k) = \int_0^{\frac{\pi}{2}} \frac{d\theta}{\sqrt{1 - k^2 \sin^2 \theta}} \quad (14)$$

Equation (13) shows that the downwash is zero far upstream, twice α_i far downstream, and $\pm\infty$ at the lifting line. Helmbold (ref. 7) has pointed out that equation (9) is bounded by equation (13), that is, the downwash is maximized along the x -axis. This observation has practical consequences in that the destabilizing effects of the downwash are reduced if a horizontal tail or canard is placed far above or far below the main wing wake.

SOLUTION IN THE PLANE OF SYMMETRY

The downwash integral (eq. (9)) is more easily understood and solved in terms of a geometric picture (see fig. 3). The coordinate system is a right handed one with origin at the midpoint of a lifting line of semispan s ; x extends downstream; y extends out the right wing; and z is positive extending vertically up. Note that x and z are in directions opposite to those in their usual definitions for flight mechanics. This avoids sign confusion in the following derivation.

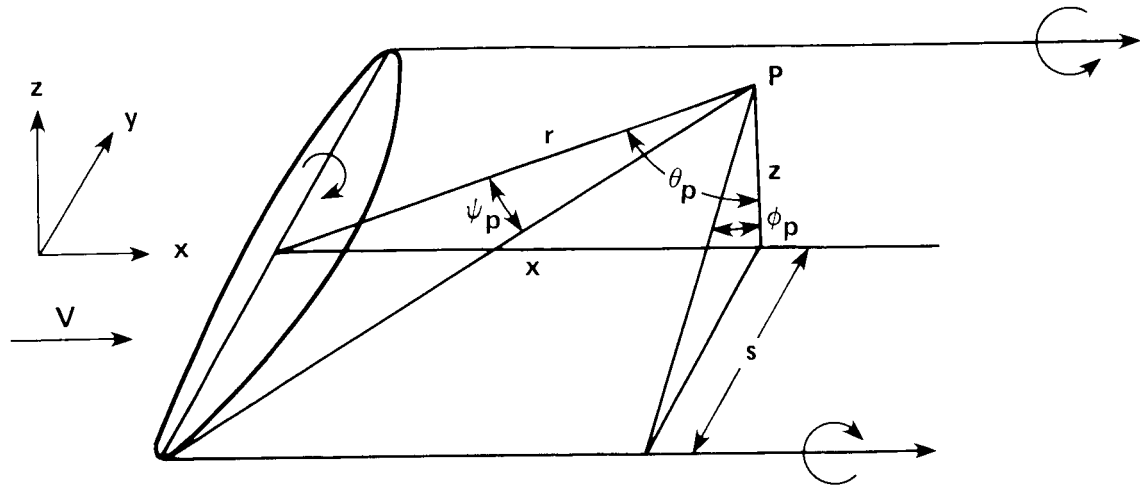


Figure 3. - Lifting line geometry.

Normalizing the length variables by the semispan s , yields the dimensionless quantities

$$\begin{aligned}
 \xi &= x/s \\
 \eta &= y/s \\
 \zeta &= z/s \\
 \rho &= r/s
 \end{aligned}
 \tag{15}$$

where $r^2 = x^2 + z^2$.

The point P , at which the downwash is desired, is specified by two coordinates, x and z . Four auxiliary variables are also needed: r is the distance from the lifting line to P ; and ψ_p , θ_p , and ϕ_p loosely correspond to the familiar Euler angles and are defined by equations (16).

$$\begin{aligned}
 \tan \psi_p &= \rho^{-1} & 0 \leq \psi_p \leq \pi/2 \\
 \tan \theta_p &= \xi/\zeta & -\pi/2 \leq \theta_p \leq \pi/2 \\
 \tan \phi_p &= \zeta^{-1} & -\pi/2 \leq \phi_p \leq \pi/2
 \end{aligned}
 \tag{16}$$

The angle θ_p also corresponds to the "angle of stagger" from early biplane theory, and $\tan \phi_p$ is also the inverse of the gap ratio, historically an

important parameter for determining the induced drag of biplanes and canards.

The solution for the entire plane of symmetry (eq. (9)) proceeds from the idea that the answer must collapse to the z-axis solution (eq. (11)) when $x = 0$ and it must collapse to the x-axis solution (eq. (13)) when $z = 0$. This can be made to happen, for example, if equation (9) can be separated into three terms, one resembling the z-axis integral (eq. (10)), one resembling the x-axis integral (eq. (12)), and one a residual integral which must be zero when either x or z is zero. With this in mind, the bracketed part of equation (9) can be rewritten successively as

$$\begin{aligned}
 [eq(9)] &= \left[\frac{x}{\sqrt{x^2 + y^2 + z^2}} \left(\frac{y^2}{x^2 + z^2} + \frac{y^2}{y^2 + z^2} \right) + \frac{y^2}{y^2 + z^2} \right] \\
 &= \left[\frac{x}{\sqrt{y^2 + r^2}} \left(\frac{y^2}{r^2} + \frac{y^2}{y^2 + z^2} \right) + \frac{y^2}{y^2 + z^2} \right] \\
 &= \left[\frac{x}{\sqrt{y^2 + r^2}} \left(\frac{y^2}{r^2} + 1 - \frac{z^2}{y^2 + z^2} \right) + \frac{y^2}{y^2 + z^2} \right] \\
 &= \left[\frac{x}{\sqrt{y^2 + r^2}} \left(\frac{y^2 + r^2}{r^2} - \frac{z^2}{y^2 + z^2} \right) + \frac{y^2}{y^2 + z^2} \right] \\
 &= \left[\frac{x}{r} \frac{\sqrt{y^2 + r^2}}{r} - \frac{xz^2}{(y^2 + z^2)\sqrt{y^2 + r^2}} + \frac{y^2}{y^2 + z^2} \right]
 \end{aligned}$$

Breaking out the integrals from equation (9) according to the last three terms above yields

$$\bar{\epsilon}_1 = -\frac{2}{\pi s} \int_0^s \frac{dy}{\sqrt{1 - \left(\frac{y}{s}\right)^2}} \left[\frac{x}{r} \frac{\sqrt{y^2 + r^2}}{r} \right] \quad (17a)$$

$$\bar{\epsilon}_2 = \frac{2}{\pi s} \int_0^s \frac{dy}{\sqrt{1 - \left(\frac{y}{s}\right)^2}} \left[\frac{xz^2}{(y^2 + z^2)\sqrt{y^2 + r^2}} \right] \quad (17b)$$

$$\bar{\epsilon}_3 = -\frac{2}{\pi s} \int_0^s \frac{dy}{\sqrt{1 - \left(\frac{y}{s}\right)^2}} \left[\frac{y^2}{y^2 + z^2} \right] \quad (17c)$$

where $\bar{\epsilon} = \bar{\epsilon}_1 + \bar{\epsilon}_2 + \bar{\epsilon}_3$.

Equations (17a) and (17c) can be immediately solved because they are very similar in form to equations (12) and (10), respectively. First turning to equation (17a) and noting that the complete elliptic integral of the second kind from equation (13) can be written in terms of the parameter ψ_p where $k = \sin \psi_p$, the first integral is

$$\bar{\epsilon}_1 = -\frac{\sin \theta_p}{\cos \psi_p} \frac{2}{\pi} E(\psi_p) \quad (18)$$

where from the geometry $x/r = \sin \theta_p$.

Equation (17c) is identical to equation (10) and hence the solution is the same as that of equation (11) except that it can be rewritten in a simpler form using the geometry of figure 3:

$$\bar{\epsilon}_3 = -(1 - |\cos \phi_p|) \quad (19)$$

Equation (17b) is more difficult to solve. Substituting equations (15) into equation (17b) yields

$$\bar{\epsilon}_2 = \frac{2}{\pi} \xi \zeta^2 \int_0^1 \frac{d\eta}{(\eta^2 + \zeta^2) \sqrt{(\eta^2 + \rho^2)(1 - \eta^2)}} \quad (20)$$

A relatively modern table of elliptic integrals (ref. 8) yields a closed form solution. Equation 213.02 of reference 8 (p. 48) gives the solution as

$$\bar{\epsilon}_2 = \frac{2}{\pi} \xi \zeta^2 \left[\frac{\Pi(\alpha^2, k)}{\sqrt{\rho^2 + 1}(\zeta^2 + 1)} \right] \quad (21)$$

where $\alpha^2 = 1/(1 + \zeta^2)$, $k^2 = 1/(\rho^2 + 1)$, and $\Pi(\alpha^2, k)$ is the complete elliptic integral of the third kind. The $\Pi(\alpha^2, k)$ term can be evaluated in terms of another tabulated function, Heuman's lambda function, according to equation 413.01 of reference 8 (p. 228):

$$\Pi(\alpha^2, k) = \frac{\pi}{2} \frac{\alpha \Lambda_0(\gamma, k)}{\sqrt{(\alpha^2 - k^2)(1 - \alpha^2)}} \quad (22)$$

where Λ_0 is Heuman's lambda function and

$$\sin \gamma = \sqrt{\frac{\alpha^2 - k^2}{\alpha^2(1 - k^2)}} \quad (23)$$

From equations (15) and (16), $\alpha = \sin \phi_p$ and $k = \sin \psi_p$. Substituting these into equation (23) and using the geometry of figure 3, one can show, surprisingly, that $\gamma = \theta_p$. Substituting into equation (22) yields

$$\Pi(\theta_p, \psi_p) = \frac{\pi}{2} \frac{\Lambda_0(\theta_p, \psi_p)}{\cos \psi_p \cdot |\cos \phi_p| \cdot \sin \theta_p} \quad (24)$$

Substituting again into equation (21) yields

$$\bar{\epsilon}_2 = \frac{2}{\pi} \xi \zeta^2 \left[\frac{1}{\sqrt{\rho^2 + 1}(\zeta^2 + 1)} \left(\frac{\pi}{2} \frac{\Lambda_0(\theta_p, \psi_p)}{\cos \psi_p \cdot |\cos \phi_p| \cdot \sin \theta_p} \right) \right]$$

After considerable algebra this simplifies to

$$\bar{\epsilon}_2 = |\cos \phi_p| \cdot \Lambda_0(\theta_p, \psi_p) \quad (25)$$

Combining equations (18), (19), and (25) gives the complete solution

$$\bar{\epsilon} = - \left\{ \frac{\sin \theta_p}{\cos \psi_p} \frac{2}{\pi} E(\psi_p) - |\cos \phi_p| \cdot [1 + \Lambda_0(\theta_p, \psi_p)] + 1 \right\} \quad (26)$$

The complete elliptic integral of the second kind, $E(\psi_p)$, and Heuman's lambda function, $\Lambda_0(\theta_p, \psi_p)$, can both be found tabulated in reference 8. Both functions are slowly changing and, therefore, highly amenable to a Taylor series approximation in a region of interest.

GENERAL CHARACTERISTICS OF THE SOLUTION

The downwash formula just derived (eq. (26)) is significant as a theoretical contribution because it is the exact solution for the downwash of an elliptical wing planform. It has practical value for estimating the downwash of real wings which are generally designed with nearly elliptical loading to obtain the benefit of low induced drag for a given span and lift. It is also valuable as general design knowledge in that the entire downwash field in the plane of symmetry can be examined for useful trends that have practical consequences in design.

A few preliminary analytical checks of the solution are appropriate. As planned, the solution in the plane of symmetry (eq. (26)) collapses to the x -axis solution (eq. (13)) with $z = 0$ and collapses to the z -axis solution (eq. (11)) with $x = 0$. The solution is symmetric about the x -axis and asymmetric about the z -axis as required by equation (9). Along the x -axis, the downwash reaches its maximum far-field value of twice the induced angle of attack at the lifting line. Above or below the x -axis the downwash decreases. These characteristics are all consistent with existing theory.

Figure 4 shows curves of constant normalized downwash ($\bar{\epsilon} = \epsilon/\alpha_i$) plotted in the plane of symmetry which has been scaled by the semispan. The abscissa is the normalized x -direction and the ordinate is the normalized z -direction. An iterative process using equation (26) has been used to generate these curves.

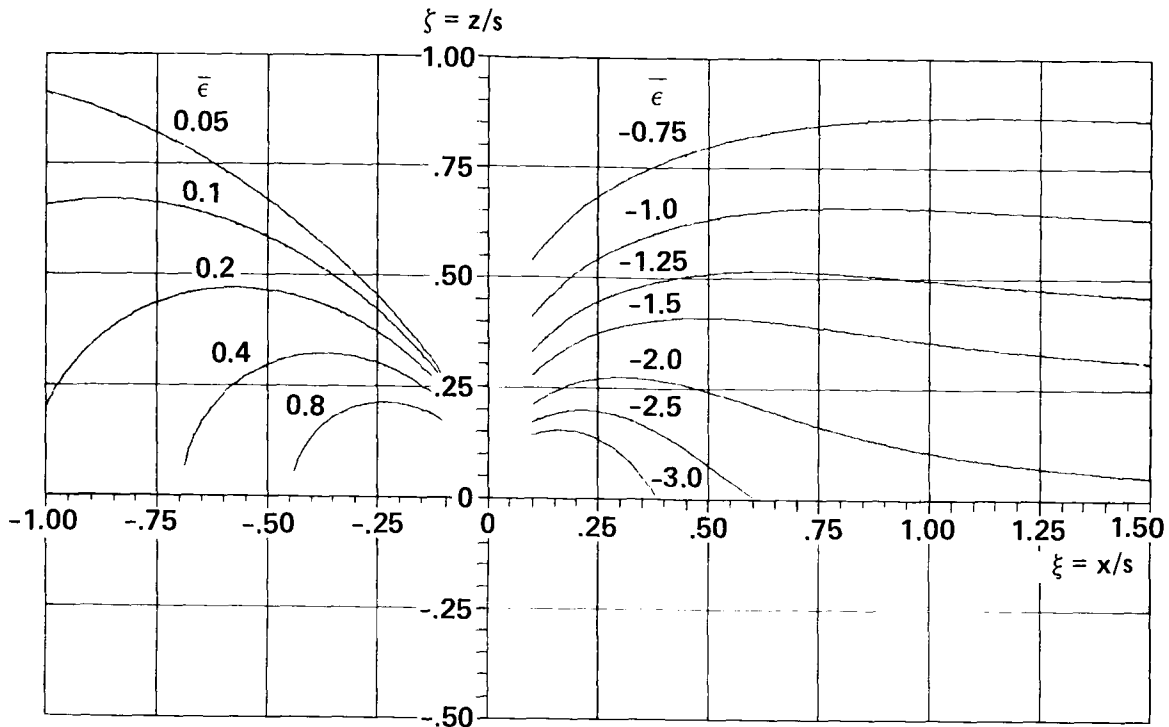


Figure 4. - Constant downwash contours.

The following general points are illustrated in figure 4. First, all the curves eventually pass through the lifting line along the ζ -axis in a manner similar to the downwash field produced by an infinite vortex line perpendicular to a uniform stream. This follows from the fact that close to the lifting line, the downwash field approaches the limit of two-dimensional flow. Second, the curve $\bar{\epsilon} = -2.0$ is a boundary between curves that intersect the positive ξ -axis and those that do not, indicating again that the maximum far-field downwash is twice the induced angle of attack at the lifting line. Third, the upwash is considerably smaller than the downwash at comparable distances upstream and downstream, respectively. This reflects the effect of the trailing vortex system on the region upstream from the wing.

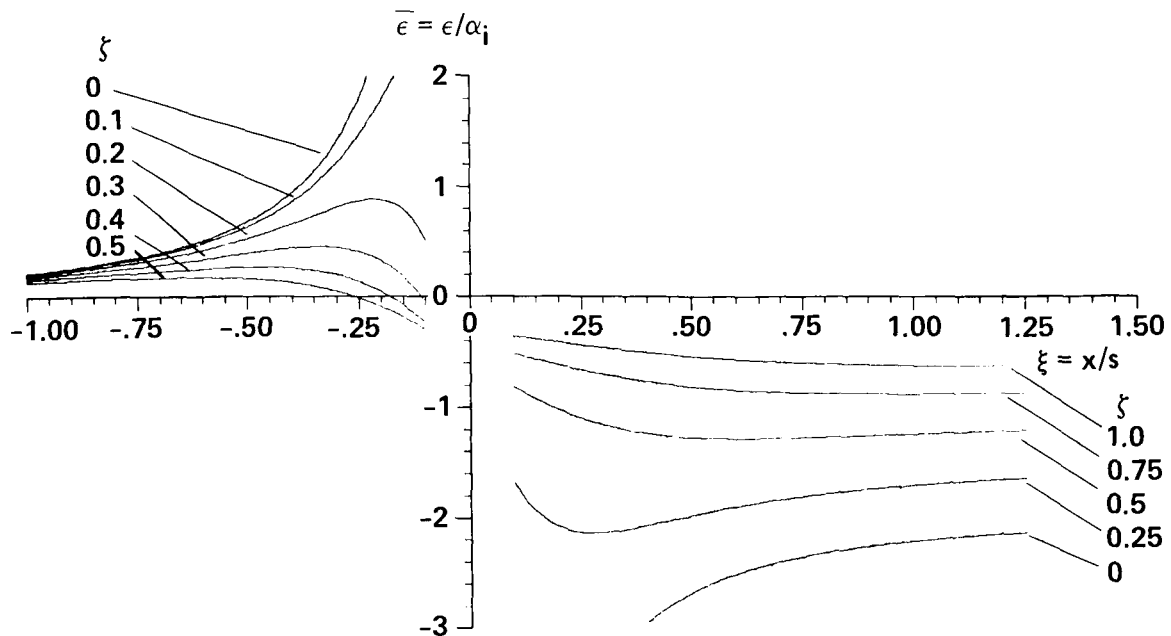


Figure 5. - Constant gap contours.

Two important trends affecting design are also evident in figure 4. First, in the normal location of a horizontal tail, that is, from $\xi = 0.5$ to $\xi = 1.5$ and from $\zeta = 0$ to $\zeta = \pm 0.5$, the downwash is a strong function of height and a mild (although not negligible) function of downstream distance. To avoid interference it is therefore desirable to place a horizontal tail as far downstream as possible and as far above or below the x -axis as possible. Second, in the upstream region of a close-coupled canard ($\xi \approx -0.5$), the upwash is a strong function of both height and upstream position. In general, placing a canard closer to the lifting line increases the upwash.

An illuminating way to present the same information contained in the previous figure is to plot downwash (\bar{c}) versus horizontal position (ξ) with curves of constant gap ratio (ζ), as shown in figure 5. This is the traditional presentation because it can be generated directly from the downwash equation, in this case, equation (26).

Figure 5 illustrates Helmbold's observation that the downwash is maximum along the x -axis. This can be seen by noting that the curve for $\zeta = 0$ bounds all the other curves. This figure also clearly shows the effect of gap ratio on the downwash. For a horizontal tail in the normal position ($\xi = 1.0$), a variation in gap ratio from 0 to 0.25 results in a downwash reduction of $\approx 23\%$.

The downwash is linearly related to the important longitudinal stability parameter, $\frac{\partial \epsilon}{\partial \alpha}$, so the trends described in this section influence directly the static longitudinal stability of airplanes.

SIMPLE APPROXIMATIONS

Since the elliptic integrals appearing in the exact solution are such slowly changing functions, keeping only a few terms of the Taylor series gives excellent results. For example, a Taylor series approximation to the complete elliptic integral of the second kind about the point $\psi_p = \pi/4$ is shown:

$$E(\psi_p) \approx 1.35064 - 0.71196 \cdot \Delta k - 0.85054 \cdot \Delta k^2 \quad (27)$$

where $\Delta k = \sin \psi_p - 0.70711$.

Heuman's lambda function can be approximated by taking a Taylor series about the point $\theta_p = 0, \psi_p = \pi/4$ and neglecting variations in ψ_p :

$$\Lambda_0(\theta_p, \psi_p) \approx [0.40093 + 0.38138 \cdot |\theta_p|] \cdot \text{sgn}(\xi) \quad (28)$$

where θ_p is in radians. Note that ξ is negative upstream and positive downstream.

A traditional approximation for the downwash (ref. 6) is a single horse-shoe vortex with reduced span and increased average circulation relative to elliptic loading such that the total circulation, as well as the total lift, is preserved. Since the total circulation of an elliptic wing is just the midspan circulation, graphically, the span loading is rectangular, with the same area underneath as that of the elliptic wing and the same height as the midspan of the elliptic wing. This occurs with a span $\pi/4$ times the elliptic

wingspan. Substituting the elliptic midspan circulation from equation (6) for Γ in equation (7), substituting $\frac{x}{s}$ for y in equation (7), and normalizing gives

$$\bar{\epsilon} = -\frac{1}{2} \left\{ \frac{\xi}{\sqrt{\xi^2 + (\frac{x}{s})^2 + \zeta^2}} \left[\frac{1}{\xi^2 + \zeta^2} + \frac{1}{(\frac{x}{s})^2 + \zeta^2} \right] + \frac{1}{(\frac{x}{s})^2 + \zeta^2} \right\} \quad (29)$$

Assuming no energy losses, the total circulation of an elliptic wing is preserved in the fully rolled up vortex sheet. Hence, equation (29) describes exactly the far downstream conditions or vanishingly low aspect ratio wings or infinitely large lift coefficients. In fact, this downwash model is often used when the wake is substantially rolled up (ref. 9). If the wake is only partially rolled up, equation (29) is still used for simplicity, but its accuracy under these conditions has not been precisely known.

Selected curves from figure 5 are repeated in figure 6 in order to compare the exact solution (eq. (26)) with the Taylor series approximation (eqs. (26)-(28)) and the fully rolled up wake model (eq. (29)). The solid lines in figure 6 represent the exact solution, the plus symbols represent the Taylor series approximation, and the dashed lines represent the fully rolled up wake approximation.

Both approximations are very accurate in the upwash region. The fully rolled up wake model is also an excellent approximation downstream (the error is less than 5%) for gaps greater than 0.25. As the gap declines from 0.25 to 0, however, the disparity with the flat-sheet solution increases until it is about 20% on the x -axis (zero gap). In comparison, the Taylor series approximation is excellent in the downwash region for small gaps, but it gradually loses accuracy for large gaps.

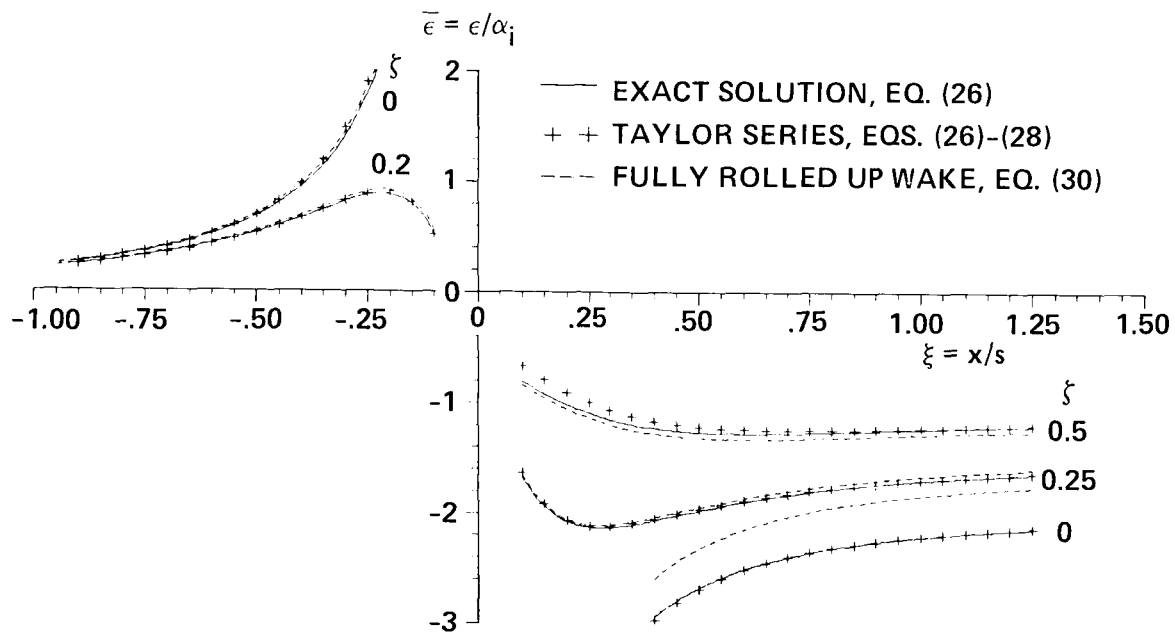


Figure 6. - Comparison of downwash formulas.

CONCLUDING REMARKS

A closed-form solution for the downwash in the plane of symmetry of an elliptically loaded line has been given (eq. (26)). The formula is derived from Prandtl's lifting-line theory and is based on the same assumptions.

This formula will describe real wing behavior most accurately in the downstream region from 1 chord behind the wing trailing edge to 1 span behind the lifting line and in the upstream region greater than 1 chord forward of the lifting line. The solution is less accurate within 1 chord of the lifting line because of the real two-dimensional airfoil distortions of the flow field, which have been neglected in using the lifting line. The solution is also less accurate far downstream because the wake has been assumed to

extend downstream as a flat sheet, when in fact it is unstable and gradually rolls up into two vortex cores. The rolling up process cannot be neglected if the aspect ratio is small ($AR < 4$) or if the lift coefficient is large ($C_L > 1.0$).

An approximation derived by simply extending the fully rolled up elliptic wing wake into the lifting line (eq. (29)), gives results within 5% of the flat-sheet solution everywhere in the plane of symmetry except downstream and close to the longitudinal (x) axis. The discrepancy between the fully rolled up wake equation and the flat-sheet solution is about 20% at its greatest and occurs on the x -axis. For rough estimates of the downwash, the fully rolled up wake model gives acceptable results which are independent of aspect ratio and lift coefficient.

Both equations (eqs. (26) and (29)) are simple one-line formulas and are therefore useful for preliminary estimates of the downwash.

Ames Research Center

National Aeronautics and Space Administration

Moffett Field, California 94035, October 5, 1984

REFERENCES

1. Glauert, H. : The Elements of Aerofoil and Airscrew Theory. Second ed., Cambridge University Press, 1948.
2. Silverstein, Abe; and Katzoff, S.: Design Charts for Predicting Downwash Angles and Wake Characteristics behind Plain and Flapped Wings. NACA Report 648, 1938.
3. McCormick, Barnes W.: Aerodynamics, Aeronautics, and Flight Mechanics. John Wiley and Sons, 1979.
4. Silverstein, Abe; Katzoff, S; and Bullivant, K. W.: Downwash and Wake behind Plain and Flapped Airfoils. NACA Report 651, 1938.
5. Fage, A.; and Simmons, L. F. G.: An Investigation of the Air-Flow Pattern in the Wake of an Aerofoil of Finite Span. Reports and Memoranda No. 951, British Aeronautical Research Committee, 1925.
6. Muttray, H.: Investigation on the Amount of Downwash behind Rectangular and Elliptical Wings. NACA TM 787, 1936.
7. Helmbold, Heinrich B.: Über die Berechnung des Abwindes hinter einem rechteckigen Tragflügel. (On the Computation of Downwash behind a Rectangular Airplane Wing.) Zeitschrift für Flugtechnik und Motorluftschiffahrt, vol. 16, no. 15, Aug. 14, 1925, pp. 291-294.
8. Byrd, Paul F.; and Friedman, Morris D.: Handbook of Elliptic Integrals for Engineers and Scientists. Springer-Verlag, New York, 1971.
9. Spreiter, John R.; and Sacks, Alvin H.: The Rolling Up of the Trailing Vortex Sheet and Its Effect on the Downwash behind Wings. J. Aeronaut. Sci., vol. 18, no. 1, Jan., 1951, pp. 21-32, 72.

1. Report No. NASA TP-2414	2. Government Accession No.	3. Recipient's Catalog No.	
4. Title and Subtitle DOWNWASH IN THE PLANE OF SYMMETRY OF AN ELLIPTICALLY LOADED WING		5. Report Date January 1985	
		6. Performing Organization Code	
7. Author(s) James D. Phillips		8. Performing Organization Report No. A-9871	
		10. Work Unit No.	
9. Performing Organization Name and Address Ames Research Center Moffett Field, Calif. 94035		11. Contract or Grant No.	
		13. Type of Report and Period Covered Technical Paper	
12. Sponsoring Agency Name and Address National Aeronautics and Space Administration Washington, DC 20546		14. Sponsoring Agency Code 532-01-11	
		15. Supplementary Notes Point of contact: James D. Phillips, Ames Research Center, M/S 210-9, Moffett Field, CA 94035 (415)694-5454 or FTS 448-5454	
16. Abstract <p>A closed-form solution for the downwash in the plane of symmetry of an elliptically loaded line is given. This theoretical result is derived from Prandtl's lifting-line theory and assumes that (1) a three-dimensional wing can be replaced by a straight lifting line, (2) this line is elliptically loaded, and (3) the trailing wake is a flat-sheet which does not roll up. The first assumption is reasonable for distances greater than about 1 chord from the wing aerodynamic center. The second assumption is satisfied by any combination of wing twist, spanwise camber variation, or planform that approximates elliptic loading. The third assumption is justified only for high-aspect-ratio wings at low lift coefficients and downstream distances less than about 1 span from the aerodynamic center.</p> <p>It is shown, however, that assuming the wake to be fully rolled up gives downwash values reasonably close to those of the flat-sheet solution derived in this paper. The wing can therefore be modeled as a single horseshoe vortex with the same lift and total circulation as the equivalent elliptically loaded line, and the predicted downwash will be a close approximation independent of aspect ratio and lift coefficient.</p> <p>The flat-sheet equation and the fully rolled up wake equation are both one-line formulas that predict the upwash field in front of the wing, as well as the downwash field behind it. These formulas are useful for preliminary estimates of the complex aerodynamic interaction between two wings (i.e., canard, tandem wing, and conventional aircraft) including the effects of gap and stagger.</p>			
17. Key Words (Suggested by Author(s)) Elliptic wing Downwash		18. Distribution Statement Unclassified - unlimited Subject Category - 02	
19. Security Classif. (of this report) Unclassified	20. Security Classif. (of this page) Unclassified	21. No. of Pages 24	22. Price* A03

National Aeronautics and
Space Administration

Washington, D.C.
20546

Official Business
Penalty for Private Use, \$300

THIRD-CLASS BULK RATE

Postage and Fees Paid
National Aeronautics and
Space Administration
NASA-451



4 2 10, A, 350107 S00161DS
DEPT OF THE AIR FORCE
ARNOLD ENG DEVELOPMENT CENTER (AFSC)
ATTN: LIBRARY/DOCUMENTS
ARNOLD AF STA TN 37389

NASA

POSTMASTER: If Undeliverable (Section 158
Postal Manual) Do Not Return
